

## CHAPTER 28

### THE DEVELOPMENT OF UNDULAR BORES WITH FRICTION

by

O Hawaleshka\* and S B Savage\*\*

#### ABSTRACT

A theoretical and experimental study of the initial development of undular bores in two-dimensional, rectangular channels with and without boundary friction was performed. Equations similar to those of Boussinesq, but including higher order and wall friction terms are presented and solved numerically by an implicit finite difference method. A Pohlhausen-type boundary layer momentum integral method is used to obtain the wall shear stress distribution under a developing long wave from the consideration of the boundary layer underneath it. The solution is performed in a quasi-iterative manner proceeding from the friction coefficient calculation for an initially assumed wave profile to the inclusion of this coefficient in the calculation of a new wave profile at an advanced time. Comparisons of theoretical and experimental results are given. For the initial development of the undular bore with which the present work is concerned, the measurements are found to be in reasonable agreement with the theoretical predictions. The effect of the wall shear stress manifests itself mainly in a slight reduction of the wave amplitudes.

---

#### INTRODUCTION

Bores are transitions between two essentially uniform liquid flows. A turbulent breaking zone is associated with "strong" bores, but if the depth change is relatively small, the bores are termed weak and may consist of a train of undular waves following the head wave. These waves are found to be closely approximated by the elliptic or cnoidal wave form of Korteweg and DeVries (1). This class of waves to which the solitary wave belongs as well is characterized by constancy of shape and a marked resistance to decay, in contrast to such waves as the non-linear shallow water waves of Airy that regardless of their initial smallness will eventually grow, steepen and break. Ursell (2) has

---

\* Assistant Professor, Mechanical Engineering Department, University of Manitoba, Winnipeg, Manitoba, Canada

\*\*Associate Professor, Department of Civil Engineering and Applied Mechanics, McGill University, Montreal, Quebec, Canada

distinguished various types of shallow water waves by the parameter  $\alpha\lambda/h^3$  where values of  $\alpha\lambda/h^3 \gg 1$ ,  $\alpha\lambda/h^3 \sim O(1)$  and  $\alpha\lambda/h^3 \ll 1$  correspond to the Airy theory, the nonlinear theory of cnoidal and solitary waves and the linearized theory respectively

Such bores may be created in many ways. For example the opening of lock gates will form positive surges in the canal and negative ones within the lock. A sudden stoppage of a turbine in a power station creates a positive surge in the supply channel and a negative one in the tail race channel. Similar bores are formed in tidal estuaries at rising tide.

It is of interest to be able to predict the development of such bores and related waves, taking account of frictional effects. Up till now, most investigations of undular bores were performed for conditions where these effects were neglected or were treated in an approximate manner by the use of, for example, some average value of a Chezy coefficient (cf. ex. Benjamin & Lighthill (3), Sandover & Taylor (4), Sandover & Zienkiewicz (5), Sturtevant (7), Peregrine (6), Murota (8)).

In this paper we treat the problem of an undular surge or an arbitrary long wave, considering the effect of boundary friction. This shear effect is obtained from the computation of the development of the boundary layer underneath the advancing wave.

#### EXPERIMENTAL SETUP AND PROCEDURE

An aluminum channel with glass side walls was used during the tests, (fig 1). Its dimensions are 30 feet length, 12 inches wide and 18 inches deep, and was typically filled to a depth of four inches of water. A close-fitting piston with a maximum stroke of three feet and with a continuously variable velocity was installed at one end of the channel and was actuated hydraulically. It was found that with suitable combinations of piston stroke, speed and water depth a complete range of bores as well as a reasonable approximation to a solitary wave could be produced. Care was taken to provide seals around the wetted portion of the piston, effectively eliminating leaks.

The surface profiles resulting from the motion of this piston were measured at several stations along the channel by streamlined, immersed, variable-resistance probes and recorded together with the piston motion on a six channel recorder. Electronic filters were used to remove unwanted higher frequencies from the signals. The wave-measuring equipment was built by Kempf-Remmers. The accuracies obtained were essentially limited by the capillary effects of the water. The probes themselves were of fiberglass construction in the shape of a symmetrical streamlined profile with conducting strips on each side of the probe's leading edge. Production run calibrations were done statically before each run, since a test dynamic calibration showed no appreciable difference.

Some dye studies of the boundary layer under the advancing wave were performed to record visually the bottom boundary layer development.

Photographic records of surface profiles, in particular at the initial stages of the piston motion were taken by both still and cine cameras

The test procedure involved the measurements of the wave profiles for various non-dimensional piston speeds  $U_p$  from 0.1 to 0.5 and for still water depths ranging from two to five inches

THEORETICAL APPROACH

1 Equations of Motion

We make use of the equations derived by Su and Gardner (9) for non-linear dispersive shallow water waves. These are in non-dimensional form

$$\frac{\partial h}{\partial t} + \frac{\partial}{\partial x}(h\bar{u}) = 0 \tag{1}$$

$$\frac{\partial(h\bar{u})}{\partial t} + \frac{\partial}{\partial x} \left[ h\bar{u}^2 + \frac{h^2}{2} - \frac{h^3}{3} (\bar{u}_{xx} + \bar{u}\bar{u}_{xx} - \bar{u}_x^2) \right] \tag{2}$$

where  $h = \frac{h^*}{h_0}$ ,  $t = t^* \sqrt{\frac{g}{h_0}}$ ,  $x = \frac{x^*}{h_0}$ ,  $y = \frac{y^*}{h_0}$

$$\bar{u} = \frac{1}{h} \int_0^h \frac{u^*}{\sqrt{gh_0}} dy$$

The starred variables are dimensional and h is the local water depth, t is time, x and y are the horizontal and vertical coordinates, u is the horizontal component of velocity,  $\bar{u}$  is the depth averaged velocity, g is the gravitational acceleration and  $h_0$  is the undisturbed reference depth, see fig. 2

Equations (1) and (2) are similar to the Boussinesq equation but include the higher order terms

$$\frac{\partial}{\partial x} \left[ \frac{h^3}{3} (\bar{u}\bar{u}_{xx} - \bar{u}_x^2) \right]$$

in equation (2). We can approximately account for the effects of wall friction by the addition of the term

$$\text{Friction term} = - \frac{fh\bar{u}|\bar{u}|}{R} \tag{3}$$

to the left hand side of equation (2), where R is the dimensionless hydraulic radius at any station,

$$R = \frac{hb}{2h+b}$$

and b is the dimensionless channel width  $b/h_0$

## 2 Calculation of the friction coefficient from a Momentum Integral consideration of the boundary layer developed by a long wave

We now carry out an approximate momentum integral analysis in order to calculate the friction coefficient  $f$ , to be used for the friction term (3) which is added to equation (2). The notation in this section is somewhat different from the previous one and unless otherwise noted unstarred variables refer to physical quantities.

Consider the development of a laminar two-dimensional boundary layer under a long wave advancing with speed  $u_F$  into still water of depth  $h_0$ . In the boundary layer analysis the inviscid fluid velocity  $u_i$  is approximated as equal to the depth-averaged value obtained from the integration of the long wave equations. Fig. 3 shows the situation when brought to a quasi-steady state with respect to the wave front, and also defines the notation to be used. In this quasi-steady frame the boundary layer equations are

$$\frac{du}{dx} + \frac{dv}{dy} = 0 \quad (4)$$

$$u \frac{du}{dx} + v \frac{dv}{dy} + \frac{1}{\rho} \frac{dp}{dx} = \nu \frac{d^2u}{dy^2} \quad (5)$$

where the symbols have the usual meanings. Upon integration we obtain the common boundary layer momentum integral equation

$$\frac{d\Theta}{dx} + (2\Theta + \delta^*) \frac{1}{u_e} \frac{du_e}{dx} = + \frac{\tau_0}{\rho u_e^2} \quad (6)$$

where  $\Theta$  and  $\delta^*$  are the momentum and displacement thicknesses respectively and the wall shear stress is defined by

$$\frac{\tau_0}{\rho} = \nu \left. \frac{du}{dy} \right|_{y=0} \quad (7)$$

Equation (6) is solved by assuming a suitable form for the velocity profile in the boundary layer, a procedure first suggested by Pohlhausen. We take the fourth degree polynomial

$$\frac{u}{u_e} = f(\eta) = \frac{U_w}{U_e} - \left( \frac{U_w}{U_e} - 1 \right) (2\eta - 2\eta^3 + \eta^4); \quad \eta = \frac{y}{\delta} \quad (8)$$

which satisfies the conditions of  $f(\eta) = \frac{U_w}{U_e}$  at  $\eta = 0$ , and 1 for  $\eta = 1$ . From this we can obtain  $k_1 = k_1(x)$  and  $k_2 = k_2(x)$  as defined by

$$\Theta = k_1 \delta \quad (9)$$

$$\delta^* = k_2 \delta \quad (10)$$

We have as well

$$\frac{dU_e}{dx} = - \frac{du_i}{dx} \quad ; \quad u_e = u_w - u_i \quad (11)$$

and 
$$\frac{\tau_0}{\rho} = \frac{\nu}{S} \frac{du}{dz} \Big|_{z=0} = -\frac{\nu}{S} (2u_1) \tag{12}$$

Hence (6) becomes

$$\frac{1}{2} \frac{d\Theta^2}{dx^2} - \frac{1}{u_e} \frac{du_1}{dx} \left(2 + \frac{k_2}{k_1}\right) \Theta^2 = -2\nu k_1 \left(\frac{u_1}{u_e^2}\right) \tag{13}$$

After defining

$$\Xi = \Theta^2 \tag{14}$$

and the Reynolds Number

$$Re = \frac{h_0 \sqrt{gh_0}}{\nu} \tag{15}$$

we obtain

$$\frac{1}{h_0} \frac{d\Xi}{dx} - \frac{2}{u_e} \left(\frac{du_1}{dx}\right) \left(2 + \frac{k_2}{k_1}\right) \frac{\Xi}{h_0} = -\frac{4k_1}{Re} \left(\frac{u_1}{u_e^2}\right) \tag{16}$$

or, in non-dimensional form

$$\frac{d\tilde{\Xi}}{d\tilde{x}} - \frac{2}{\tilde{u}_e} \frac{d\tilde{u}_1}{d\tilde{x}} \left(2 + \frac{k_2}{k_1}\right) \tilde{\Xi} = -\frac{4k_1}{Re} \frac{\tilde{u}_1}{\tilde{u}_e^2} \tag{17}$$

where  $\tilde{x} = x/h_0$ ,  $\tilde{z} = z/h_0$ ,  $\tilde{u}_1 = u_1/\sqrt{gh_0}$  and  $\tilde{u}_e = u_e/\sqrt{gh_0}$

Experimental conditions define  $Re$ , and  $k_1$  and  $k_2$  are known from the assumed form of the boundary layer profile, equation (8). Equation (17) may be solved for  $\tilde{\Xi}$  and hence for  $\Theta$  and  $S$ . If we define the wall shear stress

$$\tau_0 = \frac{1}{2} \rho f u_1^2 \tag{18}$$

we may now calculate the coefficient of friction  $f$  from the equation

$$f = -\frac{4\nu}{S u_1} \tag{19}$$

The local value of  $f$  is now used in the long wave equations (1)-(3) for the computation of the development of the wave profile

### 3 Method of Solution

Assuming a suitable initial profile for the long wave we may integrate equation (17) - using a fourth order Runge-Kutta numerical integration and thence determine all the parameters of the boundary layer developing under this surge. In particular from equation (19) we obtain the friction coefficient distribution with  $x$ , corresponding to this initial profile. This friction coefficient is assumed to be constant

over the wetted perimeter across any cross-section of the flow. It is then fed into an implicit, finite central difference method of solution for equations (1)-(3), allowing the computation of a new wave profile at an incrementally advanced time. This new wave profile is then used in equation (17) to calculate a friction coefficient distribution corresponding to it. The solution proceeds in such a quasi-iterative fashion until the entire flow region of interest is covered.

A square mesh spacing of  $\Delta x = \Delta t = 0.2$  was used in most computations. The general finite differences solution followed the method outlined by Wachspress (10). The governing equations (1)-(3) are expressed as simultaneous, central (3-point) finite difference equations at each grid point at the desired time step and solved by a forward elimination, backward substitution technique (line inversion).

Special procedures are required near the starting and ending boundaries since full central differences cannot be evaluated there. To reduce computation time, we specify initially a small portion of the x-axis ( $t = 0$ ) and add new data points for the undisturbed liquid ahead of the advancing wave as it becomes necessary.

## RESULTS

Figure 4 shows the comparison of our theoretical results with and without the effect of friction. We note that the main effect of the wall shear stress manifests itself mainly in the reduction of the wave peaks. The troughs seem relatively unaffected. This is in contrast to some experimental results given by Sandover and Zinkiewicz (5) who note that the troughs become shallower as the friction increases.

The value of the friction coefficient calculated in this manner is typically of the order of  $3.0 \times 10^{-3}$  far from the head wave. At the start of the wave the friction coefficient is very large but decreases rapidly with distance from the very beginning of the wave.

Figures 5 and 6 give comparisons of experiments with theory with the friction taken into account. The agreement is generally good in particular at the lower non-dimensional piston speed  $u_0 = 0.1$ . The first peak is well described but the theory indicates lower peaks for the trailing waves. The troughs are well predicted. The agreement becomes better with increasing time. For  $u_0 = 0.2$  the agreement is less good, the theory seeming to exaggerate the actual swings of the peaks and troughs. The wavelength is well represented.

The above remarks are confirmed by figures 7 and 8, where we show the growth of the first peak and of the first wavelength from theory and experiment for cases with and without wall friction.

CONCLUSIONS

The method shown seems to reproduce the initial development of the undular bore reasonably well. It indicates the trends of behaviour regarding the influence of wall friction. For the experimental conditions described herein the effect is fairly small.

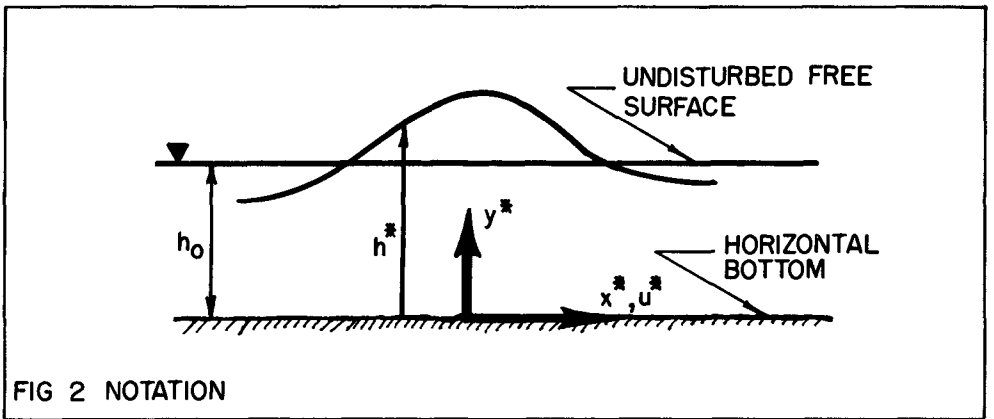
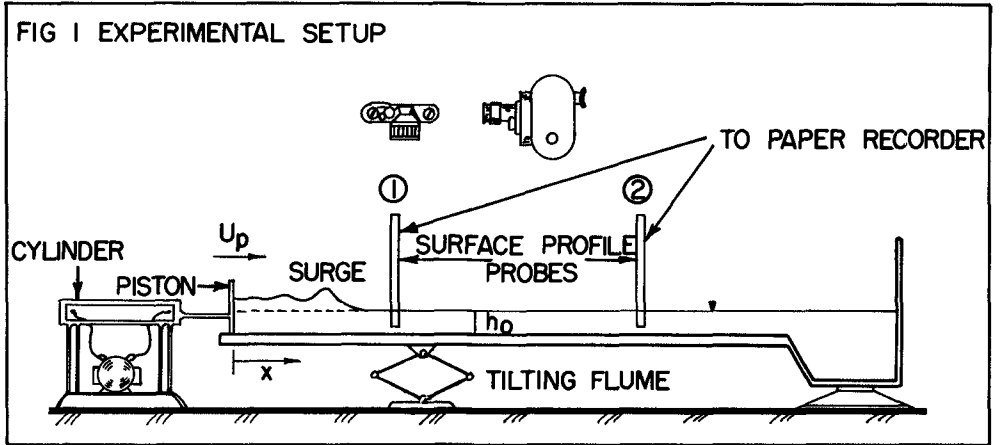
The analysis of the friction coefficient development is limited by the assumed form of the boundary layer velocity profile. It is possible that velocity reversals may appear as the wave develops and undulations become larger. These changes would invalidate the boundary layer approach described.

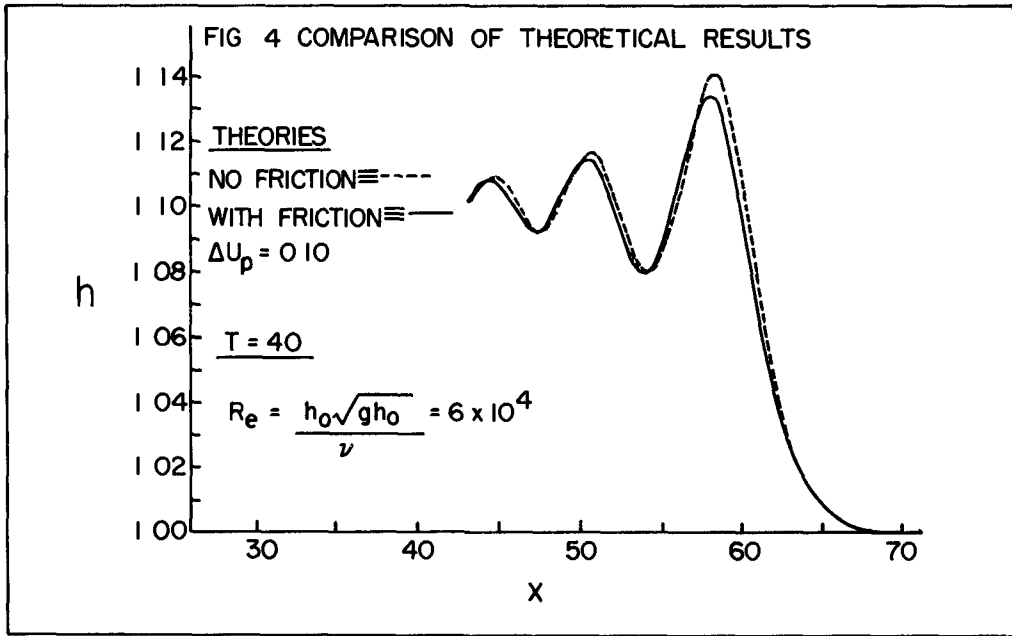
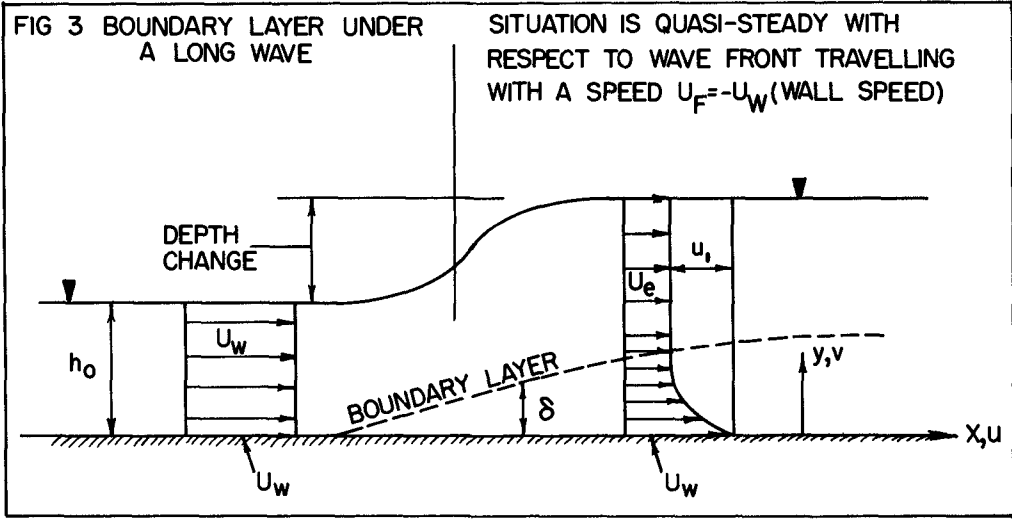
The above method (without friction) has been extended and applied successfully to various problems where the depth is variable, in particular to the development of a solitary wave crossing a bar or a trench, the solitary wave climbing a beach and to the development of an undular bore moving up a beach. These results will be given in a forthcoming paper.

BIBLIOGRAPHY

- 
- 1 Korteweg, D J & deVries, G , 1895, Phil Mag (V), 39, 422-443
  - 2 Ursell, F , 1953, The Long-Wave Paradox in the Theory of Gravity Waves, Proc Camb Phil Soc 39, 685-694
  - 3 Benjamin, T B & Lighthill, M J , 1954, On Cnoidal Waves and Bores, Proc Roy Soc A, 224, 448-60
  - 4 Sandover, J A & Taylor, C , 1962, La Houille Blanche, 17, 443-455
  - 5 Sandover, J A & Zinkiewicz, O C , 1957, Experiments on surge waves, Water Power, 9, 418-424
  - 6 Peregrine, D H , 1966, Calculation of the Development of the Undular Bore, J Fl Mech (25), 2, 321-330
  - 7 Sturtevant, J , 1965, Implications of experiments on the weak undular bore, Phys of Fluids, vol 8, 6
  - 8 Muroka, A , 1966, Tenth Conf Coastal Engrg , 24, 382-395
  - 9 Su, C H & Gardner, C S , 1969, Derivation of the Korteweg-deVries Equation and Burger's Equation, J Math Phys ,10,3, 536-39
  - 10 Wachspress, E , 1960, Numerical Solution of Boundary Value Problems, Mathematical Methods for Digital Computers, Ralston, A & Wilf, H S ed , Wiley

=====





WAVE AMPLITUDES AT FIXED X

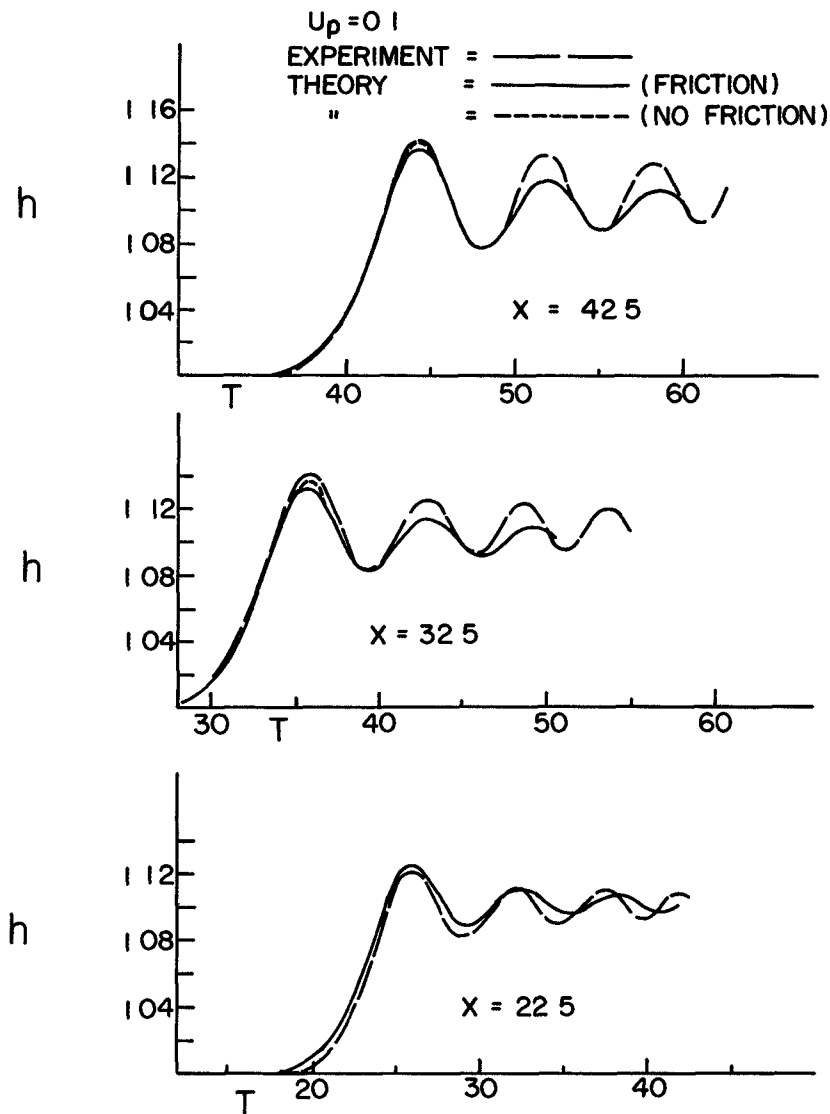


FIG 5 DEVELOPMENT OF AN UNDULAR BORE ,  $U_p = 0.1$

WAVE AMPLITUDES AT FIXED X

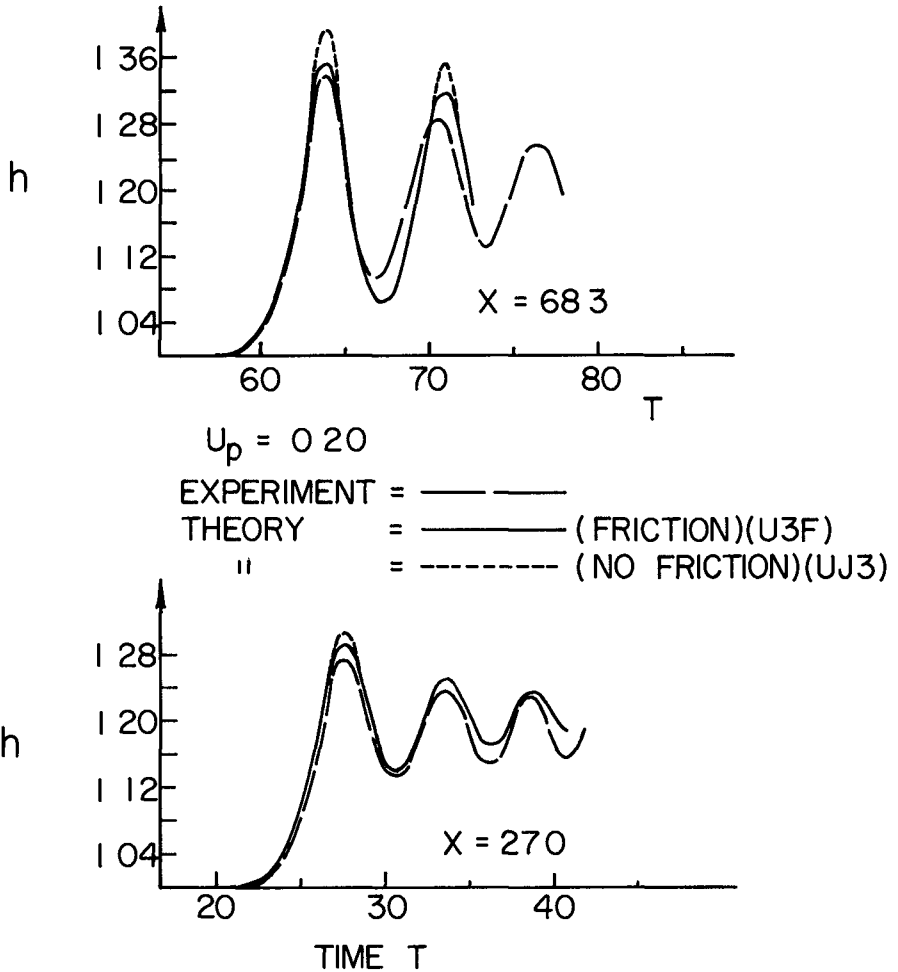


FIG 6 DEVELOPMENT OF AN UNDULAR BORE ;  $U_p = 0.2$

